Title

Ultrashort echo time adiabatic $T_{1\rho}$ (UTE-Adiab-$T_{1\rho}$) is sensitive to human cadaveric knee joint deformation induced by mechanical loading and unloading.

Authors

Jerban, Saeed
Ma, Yajun
Kasibhatla, Akhil
et al.

Publication Date

2021-07-01

DOI

10.1016/j.mri.2021.04.014

Peer reviewed

Magnetic Resonance Imaging 80 (2021) 98–105

Contents lists available at ScienceDirect

Magnetic Resonance Imaging

journal homepage: www.elsevier.com/locate/mri

Ultrashort echo time adiabatic $T_{1\rho}$ (UTE-Adiab-$T_{1\rho}$) is sensitive to human cadaveric knee joint deformation induced by mechanical loading and unloading

Saeed Jerban [a,*], Yajun Ma [a], Akhil Kasibhatla [a], Mei Wu [a], Nikolaus Szeverenyi [a], Monica Guma [b], Dana Covey [c,d], Darryl D'lima [e], Samuel R. Ward [d,f], Robert L. Sah [d,f], Eric Y. Chang [g,a], Jiang Du [a], Christine B. Chung [a]

[a] Department of Radiology, University of California, San Diego, CA, USA
[b] Department of Medicine, School of Medicine, University of California, San Diego, CA, USA
[c] Orthopaedic Service, VA San Diego Healthcare System, San Diego, CA, USA
[d] Department of Orthopedic Surgery, University of California, San Diego, CA, USA
[e] Shiley Center for Orthopedic Research and Education at Scripps Clinic, CA, USA
[f] Department of Bioengineering, University of California, San Diego, CA, USA
[g] Research Service, VA San Diego Healthcare System, San Diego, La Jolla, CA, USA

ARTICLE INFO

Keywords:
Knee
Mechanical loading
Ultrashort echo time MRI
Adiabatic $T_{1\rho}$
Cartilage
Meniscus deformation

ABSTRACT

Purpose: The development of ultrashort echo time (UTE) MRI sequences has led to improved imaging of tissues with short T_2 relaxation times, such as the deep layer cartilage and meniscus. UTE combined with adiabatic $T_{1\rho}$ preparation (UTE-Adiab-$T_{1\rho}$) is an MRI measure with low sensitivity to the magic angle effect. This study aimed to investigate the sensitivity of UTE-Adiab-$T_{1\rho}$ to mechanical load-induced deformations in the tibiofemoral cartilage and meniscus of human cadaveric knee joints.

Methods: Eight knee joints from young (42 ± 12 years at death) donors were evaluated on a 3 T scanner using the UTE-Adiab-$T_{1\rho}$ sequence under four sequential loading conditions: load = 0 N (Load0), load = 300 N (Load1), load = 500 N (Load2), and load = 0 N (Unload). UTE-Adiab-$T_{1\rho}$ was measured in the meniscus (M), femoral articular cartilage (FAC), tibial articular cartilage (TAC), articular cartilage regions uncovered by meniscus (AC-UC), and articular cartilage regions covered by meniscus (AC-MC) within region of interests (ROIs) manually selected by an experienced MR scientist. The Kruskal–Wallis test, with corrected significance level for multiple comparisons, was used to examine the UTE-Adiab-$T_{1\rho}$ differences between different loading conditions.

Results: UTE-Adiab-$T_{1\rho}$ decreased in all grouped ROIs under both Load1 and Load2 conditions (−18.7% and −16.9% for M, −18.8% and − 12.6% for FAC, −21.4% and − 10.7% for TAC, −26.2% and − 13.9% for AC-UC, and − 16.9% and − 10.7% for AC-MC). After unloading, average UTE-Adiab-$T_{1\rho}$ increased across all ROIs and within a lower range compared with the average UTE-Adiab-$T_{1\rho}$ decreases induced by the two previous loading conditions. The loading-induced differences were statistically non-significant.

Conclusions: While UTE-Adiab-$T_{1\rho}$ reduction by loading is likely an indication of tissue deformation, the increase of UTE-Adiab-$T_{1\rho}$ within a lower range by unloading implies partial tissue restoration. This study highlights the UTE-Adiab-$T_{1\rho}$ technique as an imaging marker of tissue function for detecting deformation patterns under loading.

Abbreviations: MR, magnetic resonance; MRI, magnetic resonance imaging; 3D, three-dimensional; UTE, ultrashort echo time imaging; UTE-Adiab-$T_{1\rho}$, adiabatic inversion recovery UTE $T_{1\rho}$; RF, radio frequency; FOV, field of view; ROI, region of interest; TE, echo time; TR, repetition time; FA, flip angle; TFC, tibiofemoral articular cartilage; M, meniscus; FAC, femoral articular cartilage; TAC, tibial articular cartilage; FAC-MC, femoral articular cartilage covered by meniscus; FAC-UC, femoral articular cartilage uncovered by meniscus; TAC-MC, tibial articular cartilage covered by meniscus; TAC-UC, tibial articular cartilage uncovered by meniscus; AC-MC, articular cartilage regions covered by meniscus; AC-UC, articular cartilage regions uncovered by meniscus; PG, proteoglycan.

* Corresponding author at: Department of Radiology, University of California, 9500 Gilman Drive, San Diego, CA 92093, USA.
E-mail address: sjerban@ucsd.edu (S. Jerban).

https://doi.org/10.1016/j.mri.2021.04.014
Received 1 November 2020; Received in revised form 13 April 2021; Accepted 29 April 2021
Available online 2 May 2021

1. Introduction

The articular cartilage and meniscus, two crucial components of the human knee joint, are under compressive mechanical load during walking and standing [1,2]. The articular cartilage lines the surfaces of tibial and femoral osteochondral bone to facilitate joint articulation [1,3], while the meniscus plays a significant role in absorbing mechanical shock and in facilitating load transfer between the femur and tibia [2]. Approximately 60–70% of the dry weight of the cartilage and meniscus is comprised of collagen [1–3]. One of the most prevalent diseases that affects the knee joint is osteoarthritis (OA), a degenerative condition that breaks down the cartilage and other critical tissues of the joint [4,5]. Patients with advanced OA may be unable to perform the usual activities of daily living and often require serious medical interventions, such as surgery, that result in increased national health care costs [6].

Due to its ability to provide high resolution and high contrast images of the knee joint, magnetic resonance imaging (MRI) has been used increasingly to detect degeneration in knee joint tissues, providing morphological assessment that can aid in the diagnosis of OA. However, a large portion of these knee joint tissues, namely the meniscus and deep layer cartilage, cannot be quantitatively assessed with standard clinical morphologic MRI sequences due to their short T_2 values [7–10]. Ultrashort echo time (UTE) MRI sequences, on the other hand, are able to image musculoskeletal (MSK) tissues with high signal [10–18]. Using UTE MRI, signal can be acquired after radiofrequency (RF) excitation—as quickly as is allowed by the RF hardware (e.g., 32 μs)—before any major transverse magnetization decay. However, even when leveraging the ability of UTE MRI to image these MSK tissues with short T_2 relaxation times, the quantitative MRI biomarkers, such as $T_{1\rho}$, T_2, and T_2* are still sensitive to the tissue's orientation angle in the scanner, i.e., the magic angle effect [19–21].

It has been hypothesized that $T_{1\rho}$ relaxation time is sensitive to the slow-motion interactions between protons of water molecules and protons of proteoglycan (PG) macromolecules in the articular cartilage and meniscus [22–24]. A novel three-dimensional UTE $T_{1\rho}$ sequence that uses an adiabatic spin-lock pulse cluster followed by Cones data acquisition (3D UTE-Adiab-$T_{1\rho}$) has recently been developed [25]. The adiabatic pulses provide robust spin locking that is insensitive to B1 inhomogeneity [25]. Furthermore, a recent study has reported significantly lower magic angle effect for this 3D UTE-Adiab-$T_{1\rho}$ sequence compared with Cones continuous wave $T_{1\rho}$ and Cones T_2* sequences performed in patellar cartilage [26], making it a strong candidate for robust quantitative MRI assessment of the articular cartilage and meniscus in the knee joint [25,27,28].

MRI-based knee investigation traditionally takes place with the patient supine, non-weight-bearing, even though this positioning does not mimic the actual physiological condition of the loaded joint. This methodology is not optimal for the detection of cartilage and meniscus degeneration during early-stage OA. It is hypothesized that changes in collagen fibrils and PG of the cartilage and meniscus that are known to occur at the early stages of OA disease progression can alter the mechanical properties of the tissue components [3,29–31]. Several MRI-based studies on knee joints have been performed under mechanical loading in an effort to better detect disease-specific changes in knee mechanics [31]. It is thought that mechanical malfunctions in the joint associated with early-stage OA degeneration of the cartilage and meniscus may be unmasked in distinct deformation patterns under known mechanical loads. In most reported MRI-based knee-loading studies, subjects are assessed while lying in a supine position inside a standard clinical scanner while the mechanical load is applied to their feet using an MRI-compatible loading device [32–53].

The loading-induced changes in conventional $T_{1\rho}$ values of cartilage have been studied in the literature and resulted in contradictory reports. Several studies have shown a decreasing trend of $T_{1\rho}$ during loading, with an increasing trend during unloading [44,49], whereas other studies have demonstrated $T_{1\rho}$ increases during loading, with decreases during unloading [54–56]. Similar studies done in the meniscus have reported an increasing trend in $T_{1\rho}$ values of meniscus during loading [50,51].

The main objective of this study was to investigate the sensitivity of the UTE-Adiab-$T_{1\rho}$ biomarker to tibiofemoral cartilage and meniscus deformation in human cadaveric knee joints during mechanical loading. Tissues undergoing an increasing load step were hypothesized to demonstrate decreasing $T1_\rho$ values associated with extracellular matrix (ECM) compaction, altered fiber orientation, and subsequent dynamic water shift in tissues.

This feasibility study provides a basis for future in vivo studies focused on detecting potential mechanical malfunction in early-stage OA knee joints.

2. Materials and methods

2.1. Mechanical loading device

An MRI-compatible loading device was manufactured from polyvinyl chloride (PVC) tubes, high-density polyethylene (HDPE) plates, and nylon bolts and screws. Fig. 1A shows the final prototyped loading device with a wrapped, mounted knee joint. Eight sets of plastic springs (Ultem* PEI resin, LL100125U40G, Lee Spring, NY, USA) with known stiffness were used and the applied compression load was manually adjustable using a 1-in. nylon screw. The applied load was calculated by multiplying the spring stiffness by the average spring deformation length (calculated by the operator using a plastic measure during MRI scans). The average stiffness of springs was 3.2 N/mm, as measured and reported by the manufacturer.

2.2. Sample preparation

Eight normal, fresh-frozen human knee joints from relatively young (42 ± 12 years at death) donors were acquired from a non-profit donation company (United Tissue Network, Phoenix, AZ). Frozen knee joints underwent one freeze-thaw cycle before scanning and were imaged using a 2D x-ray scanner to confirm that the joint space width was normal. No joint-related diseases were recorded for the donors before death. The proximal and distal shafts (femoral and tibial) were cut in order to fit the joints into the loading device. The final length of each joint was approximately 30 to 40 cm (Fig. 1). The tibia holder of the loading device (left black cylinder in Fig. 1A) was vertically adjusted using the connecting screws and a set of holes drilled at different heights on the HDPE plate. We attempted to avoid knee flexion during loading by properly adjusting the joint alignment before scanning. Moreover, dense polyfoam pads were placed within the MRI coil on top of the joint to prevent potential flexion. No significant flexion of the joints was observed in this study.

Each of the cadaver joints was wrapped in biohazard absorbent pads and then sealed before being placed in the loading device.

2.3. UTE MRI scans and mechanical loading

The following three loading conditions were applied for all eight knee specimens: Load = 300 N (Load1), Load = 500 N (Load2), and Load = 0 N (Unload), while only the last four scanned specimens underwent an additional fourth scan at baseline (Load0). A 20-min rest period was included between each loading condition, which was initially assumed to be an adequate amount of time for tissue restoration. The Load0 scans were omitted for the first four specimens in an effort to reduce the total scan time. While the Load0 results were initially assumed to be similar to the Unload results, this was questioned after analyzing the first four scanned specimens and was subsequently found to be incorrect after analyzing the remaining four scanned specimens.

Knee joints mounted in the loading device were placed parallel to B0 and scanned on a clinical 3 T MR scanner (MR750, GE Healthcare Technologies, WI, USA) in the sagittal plane using an eight-channel transmit/receive knee coil at room temperature (~20 °C). For each loading stage, the UTE-Adiab-$T_{1\rho}$ sequence was repeated seven times with different pairs of adiabatic full passage (AFP) pulses including 0, 2, 4, 6, 8, 12, and 16 pulses, corresponding to spin-locking times (TSLs) of 0, 12, 24, 36, 48, 72, and 96 ms, respectively, in addition to the standard fat saturation pulse. Other imaging parameters included: TR = 500 ms, TE = 0.032 ms, FA = 10°, number of spokes per adiabatic preparation = 25, and an approximate scan time of 5 min for each TSL. Field of view (FOV), matrix dimension, nominal in-plane pixel size, slice thickness, slice number, and the total scan time were 140 × 140 mm^2, 256 × 256 × 40, 0.54 × 0.54 mm^2, and 2 mm, 40, and 35 min, respectively. The pulse sequence diagram of the UTE-Adiab-$T_{1\rho}$ sequence is shown in Fig. 1B, with additional details on the sequence given in an earlier study by Ma et al. [25]. In $T_{1\rho}$ imaging, the relatively long TSL with low power locks the magnetization vector into a rotated frame that helps maintain the spinning protons in phase [22–24]. It should be noted that all joints were also scanned using clinical standard MRI sequences (proton density-weighted and T_2 fat saturation) in order to confirm that the cartilage and menisci were normal.

2.4. MRI data analysis

Five ROIs were defined on UTE-Adiab-$T_{1\rho}$ images (TSL = 12 ms) at the lateral and medial compartments (one central slice for each compartment) of the knee joints for $T_{1\rho}$ analysis. ROIs were selected by an MRI scientist with two years of experience with MR knee analysis. Fig. 1C schematically depicts drawn ROIs on the medial compartment of a representative knee joint (44-year-old-female). The following individual ROIs were generated for analysis: meniscus (M), femoral articular cartilage covered by meniscus (FAC-MC), tibial articular cartilage covered by meniscus (TAC-MC), femoral articular cartilage uncovered by meniscus (FAC-UC), and tibial articular cartilage uncovered by meniscus (TAC-UC). These individual ROIs were also combined in various pairings to form four additional grouped ROIs for analysis: 1) femoral articular cartilage (FAC): FAC-MC and FAC-UC; 2) tibial articular cartilage (TAC): TAC-MC and TAC-UC; 3) articular cartilage region covered by meniscus (AC-MC): FAC-MC and TAC-MC; and 4) articular cartilage region uncovered by meniscus (AC-UC): FAC-UC and TAC-UC.

2.5. Statistical analysis

UTE-Adiab-$T_{1\rho}$ values were compared between the sequential loading conditions (Load1, Load2, and Unload) for all eight specimens, with an additional comparison between the Load0 and Load1 datasets for the last four specimens, within M, FAC, TAC, AC-MC, and AC-UC ROIs. Performing the one-sample Kolmogorov-Smirnov test showed that the measured $T_{1\rho}$ values in this study were not normally distributed, so the Kruskal–Wallis test by ranks was used to examine data differences between the four loading conditions (Load0, Load1, Load2, and Unload).

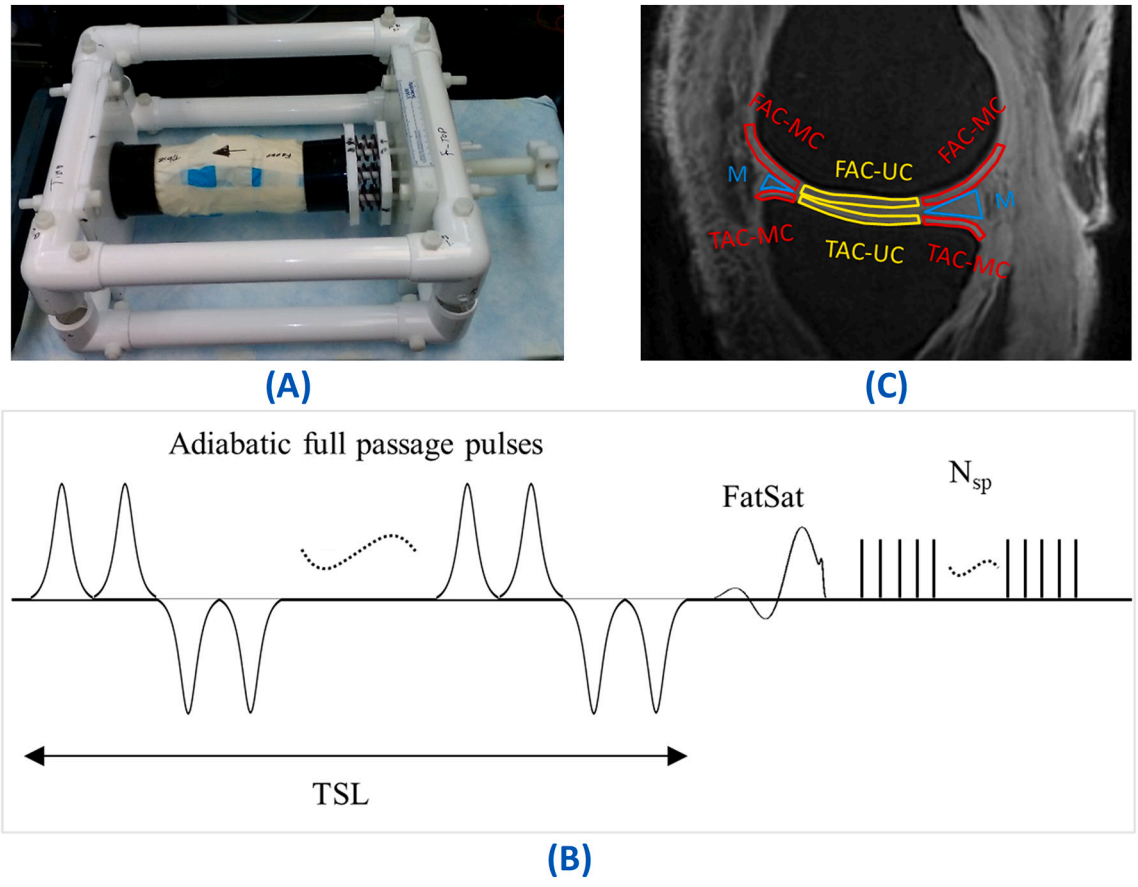

Fig. 1. (A) Designed and fabricated MRI-compatible loading device using polyvinyl chloride (PVC) tubes, high-density polyethylene (HDPE) plates, and nylon bolts and screws. The load was manually adjusted by an axially installed nylon screw compressing eight plastic springs. The applied load was monitored by measuring the length of the springs. (B) Pulse sequence diagram of the 3D UTE cones with fully passage adiabatic $T_{1\rho}$ (UTE-Adiab-$T_{1\rho}$) and standard fat saturation preparations used in this study. For each cluster of preparation pulses, a number of spiral spokes (Nsp) were acquired using UTE cones with a minimal nominal TE of 32 μs. TSL refers to spin-locking time. (C) Schematic regions of interest (ROIs) defined at the lateral compartment of a representative cadaveric knee joint (44-year-old-female). M refers to meniscus. FAC-MC and TAC-MC refer to femoral and tibial articular cartilage covered by meniscus. FAC-UC and TAC-UC refer to femoral and tibial articular cartilage uncovered by meniscus.

P-values below 0.05 were considered as significant. The Holm–Bonferroni method was used to correct the significance level for multiple comparisons. UTE-MRI measurements and statistical analyses were performed using MATLAB (version 2017, The Mathworks Inc., Natick, MA, USA) codes developed in-house.

3. Results

Fig. 2 shows UTE-Adiab-$T_{1\rho}$ pixel maps of the tibiofemoral cartilage and meniscus of a representative human cadaveric knee joint (44-year-old-female) under the four loading conditions (Load0, Load1, Load2, and Unload). UTE-Adiab-$T_{1\rho}$ demonstrated an obvious decrease under the first (Fig. 2B) and second loading steps (Fig. 2C), while it showed a partial increasing pattern by unloading (Fig. 2D). The UTE-Adiab-$T_{1\rho}$ map before loading is uniform over the posterior femoral cartilage which is an indication of the low sensitivity to magic angle effect.

Average and standard deviation values of UTE-Adiab-$T_{1\rho}$ within five different sets of ROIs (M, FAC, TAC, AC-MC, and AC-UC) averaged over lateral and medial joint compartments, and under the four loading conditions, are presented in Table 1. As mentioned previously, values for the Load0 dataset were only measured and calculated for the last four knee joints.

Average percentage differences of UTE-Adiab-$T_{1\rho}$ between the different loading conditions (Load1 vs. Load0, Load2 vs. Load1, and Unload vs. Load2) are presented in Table 2. Average UTE-Adiab-$T_{1\rho}$ decreased in all grouped ROIs under first loading step (−18.7, −18.8, −21.4, −26.2, and − 16.9% for M, FAC, TAC, AC-UC, and AC-MC regions, respectively, measured for last four knee joints. UTE-Adiab-$T_{1\rho}$ decreased again when the applied mechanical load increased from 300 N to 500 N for all grouped ROIs (−16.9, −12.6, −10.7, −13.9, and −10.7% for M, FAC, TAC, AC-UC, and AC-MC, respectively). Average UTE-Adiab-$T_{1\rho}$ increased in all studied regions after unloading, but within a lower range compared with average UTE-Adiab-$T_{1\rho}$ decreases induced by the preceding two loading steps. The Kruskal–Wallis test with corrected significance levels for multiple comparisons showed that all the loading and unloading induced changes in UTE-Adiab-$T_{1\rho}$ were statistically non-significant. However, the significance level was higher for changes induced by loading (Load1 vs. Load0 and Load2 vs. Load1) than those induced by unloading (Unload vs. Load2). The percentage differences in UTE-Adiab-$T_{1\rho}$ was slightly higher for AC-UC than AC-MC.

Fig. 3 shows the box and whisker plots for average UTE-Adiab-$T_{1\rho}$ within five different ROIs (M, FAC, TAC, AC-MC, and AC-UC) under the four loading conditions (Load0, Load1, Load2, and Unload).

Table 1
Average UTE-Adiab-$T_{1\rho}$ within five ROIs under four loading conditions.

	UTE-Adiab-$T_{1\rho}$ (ms)			
	Load0*	Load1	Load2	Unload
M	30.0 ± 4.1	30.5 ± 15.0	25.3 ± 4.7	28.8 ± 14.1
FAC	54.8 ± 7.4	46.2 ± 15.4	40.4 ± 9.2	43.8 ± 13.1
TAC	52.3 ± 10.8	42.4 ± 13.4	37.8 ± 9.7	43.3 ± 16.4
AC-UC	54.8 ± 12.3	40.1 ± 11.4	36.0 ± 8.6	40.6 ± 14.3
AC-MC	52.9 ± 7.5	45.5 ± 15.6	40.7 ± 9.7	45.0 ± 14.8

- Meniscus (M), femoral articular cartilage (FAC), tibial articular cartilage (TAC), articular cartilage uncovered with meniscus (AC-UC), and articular cartilage covered with meniscus (AC-MC).
* Load0 datasets were only acquired for four knee joints (datasets from the other three loads were acquired for all eight joints).

Table 2
Average percentage differences of UTE-Adiab-$T_{1\rho}$ within meniscus and cartilage regions between different loading conditions.

		UTE-Adiab-$T_{1\rho}$ Diff (%)	
	L0-L1 Diff (%) *	L1-L2 Diff (%)	L2-UnL Diff (%)
M	−18.7 ($p = 0.03$)	−16.9 ($p = 0.11$)	13.6 ($p = 0.96$)
FAC	−18.8 (p = 0.07)	−12.6 ($p = 0.07$)	8.4 ($p = 0.48$)
TAC	−21.4 ($p = 0.05$)	−10.7 ($p = 0.15$)	14.3 ($p = 0.23$)
AC-UC	−26.2 (p = 0.05)	−13.9 ($p = 0.06$)	12.7 ($p = 0.32$)
AC-MC	−16.9 (p = 0.07)	−10.7 ($p = 0.13$)	10.7 ($p = 0.30$)

- Meniscus (M), femoral articular cartilage (FAC), tibial articular cartilage (TAC), articular cartilage uncovered with meniscus (AC-UC), and articular cartilage covered with meniscus (AC-MC).
* L0-L1 Diff was only calculated for four knee joints because Load0 datasets were only acquired for four knee joints.

4. Discussion

The most important finding of this study is that the UTE-Adiab-$T_{1\rho}$ biomarker can quantitively detect deformations in the articular cartilage and meniscus of the knee joint under mechanical loading. The UTE-Adiab-$T_{1\rho}$ biomarker has been introduced previously as a robust MRI-based quantification for the articular cartilage, which has a relatively long T_2, and meniscus, which has a relatively short T_2 [25]. Moreover, UTE-Adiab-$T_{1\rho}$ has demonstrated low sensitivity to the angle of tissue orientation in the MRI scanner (i.e., the magic angle effect) [27].

This study showed that UTE-Adiab-$T_{1\rho}$ is an MRI biomarker sensitive to the deformation in knee joint tissues induced by mechanical loading and unloading. UTE-Adiab-$T_{1\rho}$ reduction was detected in all studied ROIs by both loading steps (Load1 and Load2, or 300 and 500 N, respectively). UTE-Adiab-$T_{1\rho}$ decreased by at least 16.9% for the first loading step, then decreased by at least an additional 10.7% for the second loading step (Table 2, Fig. 3). The $T_{1\rho}$ reduction by loading implies tissue deformation associated with ECM compaction, altered fiber orientation, and dynamic water shift in the cartilage and meniscus. Unloading the knee joints resulted in an increase of $T_{1\rho}$ of at least 8.4%.

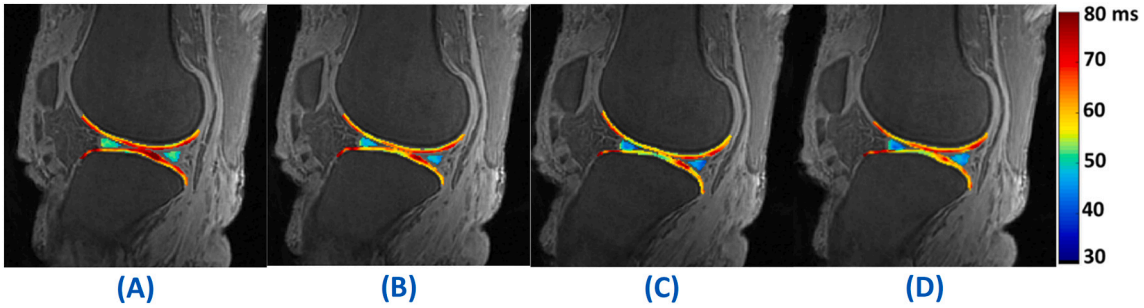

Fig. 2. UTE-Adiab-$T_{1\rho}$ pixel maps on a sagittal slice (overlaid on UTE-Adiab-$T_{1\rho}$ image, TR = 500 ms, TSL = 12 ms, and TE = 0.032 ms) at the lateral compartment of a representative cadaveric knee joint (44-year-old-female) under four different loading conditions; (A) Load0, (B) Load1, (C) Load2, and (D) Unload. The UTE-Adiab-$T_{1\rho}$ map before loading is fairly uniform over the posterior femoral cartilage which is an indication of the low magic angle effect. UTE-Adiab-$T_{1\rho}$ has decreased by load application (i.e., 300 N). UTE-Adiab-$T_{1\rho}$ experienced another reduction when the load magnitude increased from 300 to 500 N. UTE-Adiab-$T_{1\rho}$ eventually increased to higher values upon unloading.

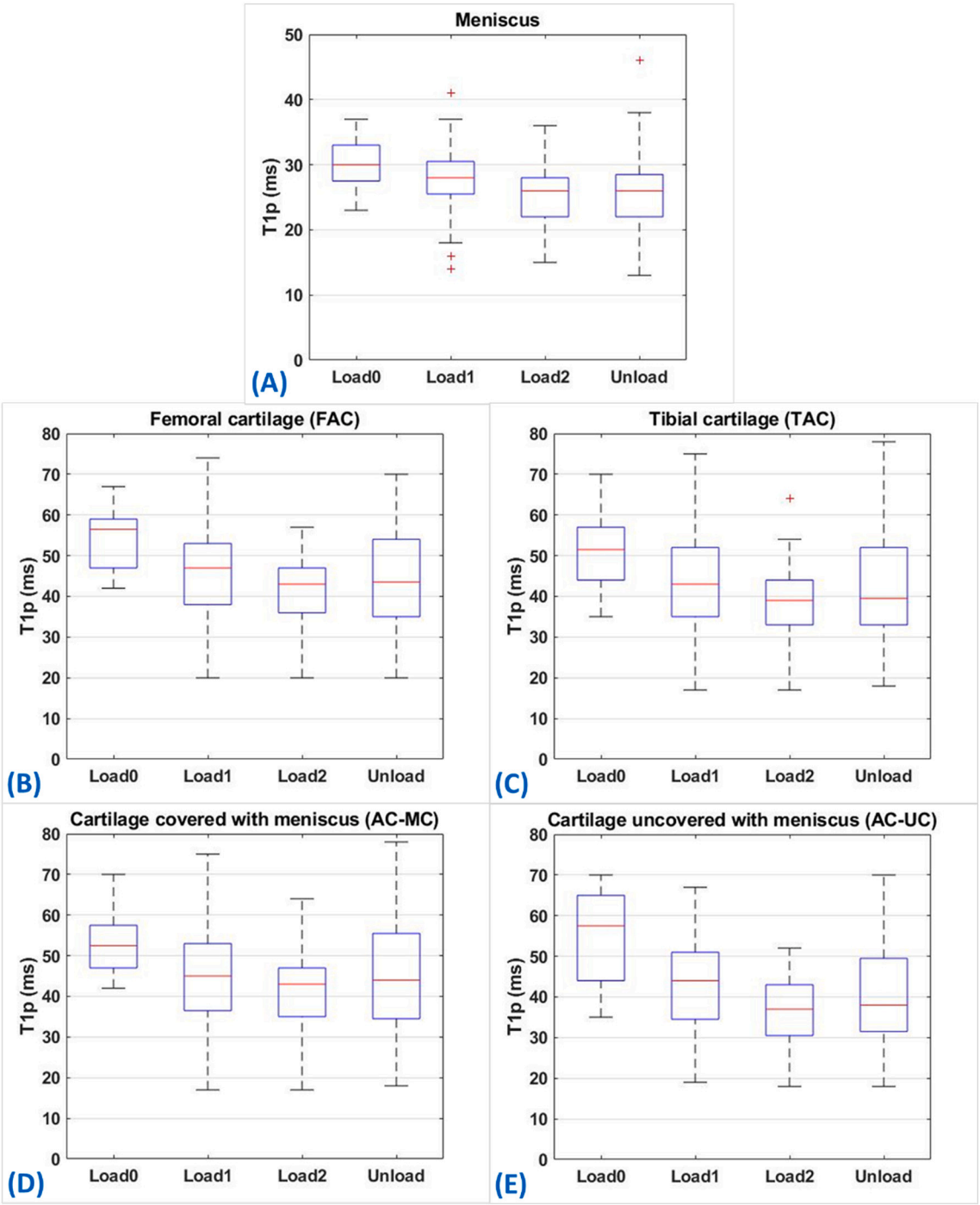

Fig. 3. Box and whisker plots of average UTE-Adiab-$T_{1\rho}$ in (A) meniscus (M), (B) femoral cartilage (FAC), (C) tibial cartilage (TAC), (D) cartilage covered with meniscus (AC-MC), and (D) cartilage uncovered with meniscus (AC-UC) under four loading conditions (Load0, Load1, Load2, and Unload). Load0 results were only calculated for four knee joints. The central mark in boxplots indicates the median, while the bottom and top edges of the boxes indicate the 25th and 75th percentiles, respectively. The '+' symbol refers to outliers. Average $T_{1\rho}$ decreased by the two loading steps, then increased by unloading.

The UTE-Adiab-$T_{1\rho}$ increase by unloading was likely caused by a partial tissue restoration associated with water absorption.

Because this was a cadaveric study, neither the cartilage nor meniscus could restore their original shapes after unloading, particularly given the limited rest time between loading steps (i.e., 20 min). According to the literature, a much longer recovery time is required for sufficient tissue restoration [57]. Complete tissue restoration would require adequate synovial fluid and blood circulation in the knee joint. Average UTE-Adiab-$T_{1\rho}$ values were at least 15% lower in all studied ROIs in the final unloading condition (Unload) compared with the initial Load0 dataset (measured for only four specimens with Load0). Such delayed tissue restoration would be much more limited for in vivo studies.

Delayed gadolinium-enhanced T_1 (T_{1Gd}), T_2, and conventional $T_{1\rho}$ are other quantitative MRI measures that have been used in previous knee loading studies [31,33,44,48,49,58–60]. However, these alternative imaging techniques are limited in two aspects: First, clinical standard morphologic MRI techniques are incapable of accurately imaging tissues with short T_2 relaxation times, such as the meniscus and the deep layer cartilage, which show as little or low signal when imaged with

clinical standard MRI sequences that use echo times that are too long [7–10]. Second, some of these MRI measures, including T_2 and conventional $T_{1\rho}$, are orientation-sensitive, so their values can be significantly changed by simple alteration of the tissue's orientation angle in the MRI scanner [20,61–63]. This phenomenon has been explained by the magic angle effect [20,26,61–63].

Souza et al. studied the effects of loading on $T_{1\rho}$ relaxation times in human tibiofemoral cartilage of OA ($n = 20$) and control ($n = 10$) knees [44]. They found significant reductions of $T_{1\rho}$ at the medial joint under mechanical loading for both OA (~12%) and control (~9%) groups. Later, they repeated the study in larger groups of normal and OA human subjects ($n = 137$) [49] and found that $T_{1\rho}$ reduction was greater for subjects with OA (13–19%) when compared to healthy controls (3–13%). The downward trend of loading-induced changes in $T_{1\rho}$ was similar to our study, but despite our study's use of a similar range of applied load, the range of UTE-Adiab-$T_{1\rho}$ reduction that we observed (17–26%) was higher than that reported in the literature [44,49]. On the contrary, Nebelung et al. reported an increasing trend of $T_{1\rho}$ when loading intact and degenerated human cartilage specimens [54,55]. During unloading, they reported a slight increasing trend of $T_{1\rho}$ [54]. Pastrama et al. [56] also reported an increasing trend of $T_{1\rho}$ in bovine cartilage during loading. These differing reports on $T_{1\rho}$ changes in cartilage are likely the results of different experimental setups, such as the use of intact whole knees [44,49] versus dissected cartilage [54–56], factors that should be examined in a future investigation.

Zonal investigation at different cartilage layers was not performed in the current study due to the limited image resolution and sample size. Subburaj et al. compared variations of conventional $T_{1\rho}$ under loading between OA (n = 20) and control individuals (n = 10) at different tibiofemoral cartilage layers [48]. They found greater $T_{1\rho}$ reductions at the superficial tibiofemoral cartilage layer (~13%) compared with the whole cartilage (~7%), whereas the deep regions showed an increase in $T_{1\rho}$. Souza et al. also reported significant decreases for $T_{1\rho}$ at the superficial layer of the cartilage, though significant increases were found at the deep layer of the cartilage performed in larger groups of participants (n = 137) [49]. Lange et al. [64] also reported $T_{1\rho}$ reduction in superficial cartilage whereas it increased in deep patellar cartilage during loading. Such zonal controversial changes in cartilage $T_{1\rho}$ might be caused by partial water movement from the superficial layer to the deep cartilage layer. Nevertheless, cartilage assessment at the deep layer using conventional $T_{1\rho}$ sequences would be challenging because the tissue may have very short T_2 relaxation times which would result in low signal to noise ratio.

Our results demonstrated a UTE-Adiab-$T_{1\rho}$ reduction pattern by loading, which is likely valid because load application is expected to compress tissue, compact the ECM, and dynamically shift water. Loading-induced differences of conventional $T_{1\rho}$ in meniscus were previously studied by Subburaj et al. [50] in OA (n = 20) and control groups (n = 10). In contrast to our results, they reported that the $T_{1\rho}$ increased in the meniscus by loading. Significantly higher variations under loading were reported for controls compared with OA subjects. Calixto et al. [51] also investigated the $T_{1\rho}$ differences under loading at three different meniscal zones of larger control ($n = 85$) and OA ($n = 39$) groups [51], reporting that $T_{1\rho}$ increased with loading for all meniscal zones for both groups. Orientation of fibers in the meniscus is likely to change from loading and compression, which could explain the controversial increasing values of the conventional $T_{1\rho}$.

UTE-Adiab-$T_{1\rho}$ and conventional $T_{1\rho}$ techniques likely share similar capabilities with regard to the assessment of tissue composition. Conventional $T_{1\rho}$ relaxation has been previously explored on bovine patellar cartilage specimens, and significant correlations were found between $T_{1\rho}$ and PG-related measures [65]. Several ex vivo studies in the literature have reported using $T_{1\rho}$ for articular cartilage assessment and have demonstrated an inverse correlation between $T_{1\rho}$ and PG content [66,67]. However, a recent study questioned the close association of $T_{1\rho}$ and PG-related measures when it showed no correlation between conventional $T_{1\rho}$ and PG content in human cartilage [68]. Other studies have shown that conventional $T_{1\rho}$ values for knee cartilage and meniscus are significantly different between control and OA patients in vivo [69,70].

This study has several limitations. First, only eight cadaveric knee joints were studied. As three to four loading conditions were applied to each knee joint specimen, the total scan time was relatively long, which limited the total number of knee joints that could be used in this feasibility study. Second, this study was performed ex vivo on cadaveric knee joints, making it difficult to extend conclusions to in vivo studies since cadaveric joints exhibit several major differences from in vivo joints, including the denaturing process, lack of muscular support for joint alignment, lack of blood and synovial fluid support, and different temperatures [71]. To further investigate UTE-Adiab-$T_{1\rho}$ as a potential measure of joint deformation under mechanical loading, future in vivo studies involving healthy, mild OA, and severe OA subjects should be performed. For future in vivo studies, the major potential challenges would be development of an active MRI-compatible loading device, consistent positioning of subjects, motion constraint, and shortening of the scan time. UTE-Adiab-$T_{1\rho}$ values are expected to be higher for in vivo studies [71] due to the higher temperatures for in vivo joints compared with this cadaveric study.

Third, the temporal differences in cartilage and meniscus under loading were not considered. Specifically, retaining constant mechanical load on the specimens is challenging due to both mechanical stress relaxations in the tissues (viscoelastic materials) and to the potential creep phenomenon of the plastic spring used in the loading device. Consequently, the applied load is expected to decrease in magnitude during the scanning period. A well-designed UTE-Adiab-$T_{1\rho}$ study utilizing an MRI-compatible pneumatic loading actuator [38,41,55,72] should be performed to account for any potential temporal differences among various knee joint tissues under loading. By using a more precise loading device with a constant load applied at each step, higher percentage differences in UTE-Adiab-$T_{1\rho}$ values are likely to be achieved. Fourth, image segmentation was performed manually on images with limited resolutions (0.54×0.54 mm^2) which may have been a challenge in obtaining accurate results for thin cartilage sites. As an alternative, high-resolution and high-contrast images (e.g., double echo steady state, DESS) could be considered for segmentation, followed by ROI registration to $T_{1\rho}$ images with lower resolution, in order to improve the segmentation process. Moreover, a deep-learning-based segmentation algorithm after adequate training would be another option to improve the segmentation process [73].

Fifth, lateral, medial, anterior, and posterior sides of the cartilage and meniscus were not considered separately in the statistical analysis (average results were used). Although these regions may have been experiencing different load magnitudes, the loading shares were not controllable using the passive loading device in this study. Moreover, at this level of consideration, load sharing between the abovementioned regions of the joint would have been affected by the anatomical differences between donors and between the left and right legs.

5. Conclusions

This study shows that UTE-Adiab-$T_{1\rho}$ is an MRI biomarker that is sensitive to the deformation in knee joint tissues induced by mechanical loading. UTE-Adiab-$T_{1\rho}$ reduction was detected in different regions of articular cartilage and meniscus under different loading conditions, which may be a sign of tissue deformation associated with ECM compaction, altered fiber orientation, and dynamic shift of water. Unloading the knee joints resulted in $T_{1\rho}$ increases in all studied ROIs, albeit at lower levels than the $T_{1\rho}$ decreases seen during loading, suggesting partial tissue restoration and inward water flux.

This study highlights the UTE-Adiab-$T_{1\rho}$ technique as a sensitive method for investigating the deformation patterns of cartilage and meniscus under mechanical loading. UTE-Adiab-$T_{1\rho}$ paired with

mechanical loading can serve as a potential tool to investigate the differences in deformation pattern between normal and abnormal knees, which will be investigated in future studies.

Declaration of Competing Interest

The authors have no conflicts of interest to declare.

Acknowledgements

The authors acknowledge grant support from national institute of health, NIH (R21AR075851, R01AR075825, 1R01NS092650, R01AR062581-06) and VA Clinical Science and Rehabilitation R&D Awards (I01CX001388 and I01RX002604). The authors also acknowledge free scan hours from GE Healthcare.

References

[1] Sophia Fox AJ, Bedi A, Rodeo SA. The basic science of articular cartilage: structure, composition, and function. Sport Heal A Multidiscip Approach 2009;1:461–8. https://doi.org/10.1177/1941738109350438.
[2] Fox AJS, Bedi A, Rodeo SA. The basic science of human knee menisci: structure, composition, and function. Sports Health 2012;4:340–51. https://doi.org/10.1177/1941738111429419.
[3] Mansour JM. Biomechanics of cartilage. Kinesiol Mech Pathomechan Hum Mov 2009:66–79. https://doi.org/10.1002/art.23548.
[4] Hayashi D, Guermazi A, Hunter DJ. Osteoarthritis year 2010 in review: imaging. Osteoarthr Cartil 2011;19:354–60. https://doi.org/10.1016/j.joca.2011.02.003.
[5] Palmer AJR, Agricola R, Price AJ, Vincent TL, Weinans H, Carr AJ. Osteoarthritis. Lancet 2015;6736:1–12. https://doi.org/10.1016/S0140-6736(14)60802-3.
[6] Yelin E, Weinstein S, King T. The burden of musculoskeletal diseases in the United States. Semin Arthritis Rheum 2016;46:259–60. https://doi.org/10.1016/j.semarthrit.2016.07.013.
[7] Gold GE, Thedens DR, Pauly JM, Fechner KP, Bergman G, Beaulieu CF, et al. MR imaging of articular cartilage of the knee: new methods using ultrashort TEs. Am J Roentgenol 1998;170:1223–6. https://doi.org/10.2214/ajr.170.5.9574589.
[8] Gatehouse PD, Bydder GM. Magnetic resonance imaging of short T2 components in tissue. Clin Radiol 2003;58:1–19. https://doi.org/10.1053/crad.2003.1157.
[9] Robson MD, Gatehouse PD, Bydder M, Bydder GM. Magnetic resonance: an introduction to Ultrashort TE (UTE) imaging. J Comput Assist Tomogr 2003;27:825–46. https://doi.org/10.1097/00004728-200311000-00001.
[10] Chang EY, Du J, Chung CB. UTE imaging in the musculoskeletal system. J Magn Reson Imaging 2015;41:870–83. https://doi.org/10.1002/jmri.24713.
[11] Du J, Bydder GM. Qualitative and quantitative ultrashort-TE MRI of cortical bone. NMR Biomed 2013;26:489–506. https://doi.org/10.1002/nbm.2906.
[12] Jerban S, Nazaran A, Cheng X, Carl M, Szeverenyi N, Du J, et al. Ultrashort echo time T2* values decrease in tendons with application of static tensile loads. J Biomech 2017;61:160–7. https://doi.org/10.1016/j.jbiomech.2017.07.018.
[13] Jerban S, Ma Y, Wong JH, Nazaran A, Searleman AC, Wan L, et al. Ultrashort echo time magnetic resonance imaging (UTE-MRI) of cortical bone correlates well with histomorphometric assessment of bone microstructure. Bone 2019;123:8–17. https://doi.org/10.1016/j.bone.2019.03.013.
[14] Jerban S, Ma Y, Wan L, Searleman AC, Jang H, Sah RL, et al. Collagen proton fraction from ultrashort echo time magnetization transfer (UTE-MT) MRI modelling correlates significantly with cortical bone porosity measured with micro-computed tomography (μCT). NMR Biomed 2019;32:e4045. https://doi.org/10.1002/nbm.4045.
[15] Jerban S, Ma Y, Nazaran A, Dorthe EW, Cory E, Carl M, et al. Detecting stress injury (fatigue fracture) in fibular cortical bone using quantitative ultrashort echo time-magnetization transfer (UTE-MT): an ex vivo study. NMR Biomed 2018;31:e3994. https://doi.org/10.1002/nbm.3994.
[16] Ma Y, Carl M, Searleman A, Lu X, Chang EY, Du J. 3D adiabatic T1ρprepared ultrashort echo time cones sequence for whole knee imaging. Magn Reson Med 2018;80:1429–39. https://doi.org/10.1002/mrm.27131.
[17] Zhu Y, Cheng X, Ma Y, Wong JH, Xie Y, Du J, et al. Rotator cuff tendon assessment using magic-angle insensitive 3D ultrashort echo time cones magnetization transfer (UTE-Cones-MT) imaging and modeling with histological correlation. J Magn Reson Imaging 2018;48:160–8. https://doi.org/10.1002/jmri.25914.
[18] Ma Y, Shao H, Du J, Chang EY. Ultrashort echo time magnetization transfer (UTE-MT) imaging and modeling: magic angle independent biomarkers of tissue properties. NMR Biomed 2016;29:1546–52. https://doi.org/10.1002/nbm.3609.
[19] Pauli C, Bae WC, Lee M, Lotz M, Bydder GM, D'Lima DL, et al. Ultrashort–Echo time MR imaging of the Patella with bicomponent analysis: correlation with histopathologic and polarized light microscopic findings. Radiology 2012;264:484–93. https://doi.org/10.1148/radiol.12111883.
[20] Shao H, Pauli C, Li S, Ma Y, Tadros AS, Kavanaugh A, et al. Magic angle effect plays a major role in both T1rho and T2 relaxation in articular cartilage. Osteoarthr Cartil 2017;25:2022–30. https://doi.org/10.1016/j.joca.2017.01.013.
[21] Chang EY, Ma Y, Du J. MR parametric mapping as a biomarker of early joint degeneration. Sport Heal A Multidiscip Approach 2016;8:405–11. https://doi.org/10.1177/1941738116661975.
[22] Le J, Peng Q, Sperling K. Biochemical magnetic resonance imaging of knee articular cartilage: T1rho and T2 mapping as cartilage degeneration biomarkers. Ann N Y Acad Sci 2016;1383:34–42. https://doi.org/10.1111/nyas.13189.
[23] Fleming BC, Biercevicz AM, Murray MM, Li W, Wang VM. Emerging techniques for tendon and ligament MRI. Magn Reson Imaging Tissue Eng 2017:209–36. https://doi.org/10.1002/9781119193272.ch10.
[24] Wang L, Regatte RR. T1ρ MRI of human musculoskeletal system. J Magn Reson Imaging 2015;41:586–600. https://doi.org/10.1002/jmri.24677.
[25] Ma Y, Carl M, Shao H, Tadros AS, Chang EY, Du J. Three-dimensional ultrashort echo time cones T 1ρ (3D UTE-cones-T 1ρ) imaging. NMR Biomed 2017;30:1–8. https://doi.org/10.1002/nbm.3709.
[26] Wu M, Ma Y, Kasibhatla A, Chen M, Jang H, Jerban S, et al. Convincing evidence for magic angle less-sensitive quantitative T 1ρ imaging of articular cartilage using the 3D ultrashort echo time cones adiabatic T 1ρ (3D UTE cones-AdiabT 1ρ) sequence. Magn Reson Med 2020;1:1–8. https://doi.org/10.1002/mrm.28317.
[27] Wu M, Kasibhatala A, Jun Ma Y, Jerban S, Chang Eric Y, Du J. Magic angle effect on adiabatic T1ρ imaging of the Achilles tendon using 3D ultrashort echo time cones trajectory. NMR Biomed 2020;30:1–10.
[28] Namiranian B, Jerban S, Ma Y, Dorthe EWEW, Masoud-Afsahi A, Wong JH, et al. Assessment of mechanical properties of articular cartilage with quantitative three-dimensional ultrashort echo time (UTE) Cones magnetic resonance imaging. J Biomech 2020. https://doi.org/10.1016/j.jbiomech.2020.110085. In Press.
[29] Juras V, Bittsansky M, Majdisova Z, Szomolanyi P, Sulzbacher I, Gäbler S, et al. In vitro determination of biomechanical properties of human articular cartilage in osteoarthritis using multi-parametric MRI. J Magn Reson 2009;197:40–7. https://doi.org/10.1016/j.jmr.2008.11.019.
[30] Desrochers J, Amrein MW, Matyas JR. Viscoelasticity of the articular cartilage surface in early osteoarthritis. Osteoarthr Cartil 2012;20:413–21. https://doi.org/10.1016/j.joca.2012.01.011.
[31] Jerban S, EY Chang E, Du J. Magnetic resonance imaging (MRI) studies of knee joint under mechanical loading: review. Magn Reson Imaging 2020;65:27–36. https://doi.org/10.1016/j.mri.2019.09.007.
[32] Mayerhoefer ME, Welsch GH, Mamisch TC, Kainberger F, Weber M, Nemec S, et al. The in vivo effects of unloading and compression on T1-Gd (dGEMRIC) relaxation times in healthy articular knee cartilage at 3.0 tesla. Eur Radiol 2010;20:443–9. https://doi.org/10.1007/s00330-009-1559-3.
[33] Nishii T, Kuroda K, Matsuoka Y, Sahara T, Yoshikawa H. Change in knee cartilage T2 in response to mechanical loading. J Magn Reson Imaging 2008;28:175–80. https://doi.org/10.1002/jmri.21418.
[34] Nebelung S, Post M, Raith S, Fischer H, Knobe M, Braun B, et al. Functional in situ assessment of human articular cartilage using MRI: a whole-knee joint loading device. Biomech Model Mechanobiol 2017;16:1971–86. https://doi.org/10.1007/s10237-017-0932-4.
[35] Wang H, Koff MF, Potter HG, Warren RF, Rodeo SA, Maher SA. An MRI-compatible loading device to assess knee joint cartilage deformation: effect of preloading and inter-test repeatability. J Biomech 2015;48:2934–40. https://doi.org/10.1016/j.jbiomech.2015.08.006.
[36] Maher SA, Wang H, Koff MF, Belkin N, Potter HG, Rodeo SA. Clinical platform for understanding the relationship between joint contact mechanics and articular cartilage changes after meniscal surgery. J Orthop Res 2017;35:600–11. https://doi.org/10.1002/jor.23365.
[37] Song Y, Greve JM, Carter DR, Koo S, Giori NJ. Articular cartilage MR imaging and thickness mapping of a loaded knee joint before and after meniscectomy. Osteoarthr Cartil 2006;14:728–37. https://doi.org/10.1016/j.joca.2006.01.011.
[38] Chan DD, Cai L, Butz KD, Trippel SB, Nauman EA, Neu CP. In vivo articular cartilage deformation: noninvasive quantification of intratissue strain during joint contact in the human knee. Sci Rep 2016;6:19220. https://doi.org/10.1038/srep19220.
[39] Neu CP. Functional imaging in OA: role of imaging in the evaluation of tissue biomechanics. Osteoarthr Cartil 2014;22:1349–59. https://doi.org/10.1016/j.joca.2014.05.016.
[40] Neu CP, Walton JH. Displacement encoding for the measurement of cartilage deformation. Magn Reson Med 2008;59:149–55. https://doi.org/10.1002/mrm.21464.
[41] Martin KJ, Neu CP, Hull ML. Quasi-steady-state displacement response of whole human cadaveric knees in a MRI scanner. J Biomech Eng 2009;131:081004. https://doi.org/10.1115/1.2978986.
[42] Chan DD, Neu CP, Hull ML. Articular cartilage deformation determined in an intact tibiofemoral joint by displacement-encoded imaging. Magn Reson Med 2009;61:989–93. https://doi.org/10.1002/mrm.21927.
[43] Chan DD, Neu CP, Hull ML. In situ deformation of cartilage in cyclically loaded tibiofemoral joints by displacement-encoded MRI. Osteoarthr Cartil 2009;17:1461–8. https://doi.org/10.1016/j.joca.2009.04.021.
[44] Souza RB, Stehling C, Wyman BT, Hellio Le Graverand MP, Li X, Link TM, et al. The effects of acute loading on T1rho and T2 relaxation times of tibiofemoral articular cartilage. Osteoarthr Cartil 2010;18:1557–63. https://doi.org/10.1016/j.joca.2010.10.001.
[45] Butz KD, Chan DD, Nauman EA, Neu CP. Stress distributions and material properties determined in articular cartilage from MRI-based finite strains. J Biomech 2011;44:2667–72. https://doi.org/10.1016/j.jbiomech.2011.08.005.
[46] Jerban S, Kasibhatla A, Ma Y, Wu M, Chen Y, Guo T, et al. Detecting articular cartilage and meniscus deformation effects using magnetization transfer ultrashort echo time (MT-UTE) modeling during mechanical load application : ex vivo feasibility study. Cartilage 2020;8:1–10. https://doi.org/10.1177/1947603520976771.

[47] Cotofana S, Eckstein F, Wirth W, Souza RB, Li X, Wyman B, et al. In vivo measures of cartilage deformation: patterns in healthy and osteoarthritic female knees using 3T MR imaging. Eur Radiol 2011;21:1127–35. https://doi.org/10.1007/s00330-011-2057-y.
[48] Subburaj K, Souza RB, Stehling C, Wyman BT, Le Graverand-Gastineau MP, Link TM, et al. Association of MR relaxation and cartilage deformation in knee osteoarthritis. J Orthop Res 2012;30:919–26. https://doi.org/10.1002/jor.22031.
[49] Souza RB, Kumar D, Calixto N, Singh J, Schooler J, Subburaj K, et al. Response of knee cartilage T1rho and T2 relaxation times to in vivo mechanical loading in individuals with and without knee osteoarthritis. Osteoarthr Cartil 2014;22:1367–76. https://doi.org/10.1016/j.joca.2014.04.017.
[50] Subburaj K, Souza RB, Wyman BT, Le Graverand-Gastineau MPH, Li X, Link TM, et al. Changes in MR relaxation times of the meniscus with acute loading: an in vivo pilot study in knee osteoarthritis. J Magn Reson Imaging 2015;41:536–43. https://doi.org/10.1002/jmri.24546.
[51] Calixto NE, Kumar D, Subburaj K, Singh J, Schooler J, Nardo L, et al. Zonal differences in meniscus MR relaxation times in response to in vivo static loading in knee osteoarthritis. J Orthop Res 2016;34:249–61. https://doi.org/10.1002/jor.23004.
[52] Patel R, Eltgroth M, Souza RB, Zhang CA, Majumdar S, Link TM, et al. Loaded versus unloaded magnetic resonance imaging (MRI) of the knee: effect on meniscus extrusion in healthy volunteers and patients with osteoarthritis. Eur J Radiol Open 2016;3:100–7. https://doi.org/10.1016/j.ejro.2016.05.002.
[53] Shiomi T, Nishii T, Tanaka H, Yamazaki Y, Murase K, Myoui A, et al. Loading and knee alignment have significant influence on cartilage MRI T2 in porcine knee joints. Osteoarthr Cartil 2010;18:902–8. https://doi.org/10.1016/j.joca.2010.05.002.
[54] Nebelung S, Sondern B, Jahr H, Tingart M, Knobe M, Thüring J, et al. Non-invasive T1ρ mapping of the human cartilage response to loading and unloading. Osteoarthr Cartil 2018;26:236–44. https://doi.org/10.1016/j.joca.2017.11.009.
[55] Nebelung S, Post M, Knobe M, Shah D, Schleich C, Hitpass L, et al. Human articular cartilage mechanosensitivity is related to histological degeneration – a functional MRI study. Osteoarthr Cartil 2019;27:1711–20. https://doi.org/10.1016/j.joca.2019.07.006.
[56] Pastrama MI, Ortiz AC, Zevenbergen L, Famaey N, Gsell W, Neu CP, et al. Combined enzymatic degradation of proteoglycans and collagen significantly alters intratissue strains in articular cartilage during cyclic compression. J Mech Behav Biomed Mater 2019;98:383–94. https://doi.org/10.1016/j.jmbbm.2019.05.040.
[57] Greaves LL, Gilbart MK, Yung A, Kozlowski P, Wilson DR. Deformation and recovery of cartilage in the intact hip under physiological loads using 7 T MRI. J Biomech 2009;42:349–54. https://doi.org/10.1016/j.jbiomech.2008.11.025.
[58] Souza RB, Baum T, Wu S, Feeley BT, Kadel N, Li X, et al. Effects of unloading on knee articular cartilage T1rho and T2 magnetic resonance imaging relaxation times: a case series. J Orthop Sports Phys Ther 2012;42:511–20. https://doi.org/10.2519/jospt.2012.3975.
[59] MacLeod TD, Subburaj K, Wu S, Kumar D, Wyatt C, Souza RB. Magnetic resonance analysis of loaded meniscus deformation: a novel technique comparing participants with and without radiographic knee osteoarthritis. Skeletal Radiol 2014;44:125–35. https://doi.org/10.1007/s00256-014-2022-3.
[60] Zevenbergen L, Gsell W, Chan DD, Vander Sloten J, Himmelreich U, Neu CP, et al. Functional assessment of strains around a full-thickness and critical sized articular cartilage defect under compressive loading using MRI. Osteoarthr Cartil 2018;26:1710–21. https://doi.org/10.1016/j.joca.2018.08.013.
[61] Fullerton GD, Cameron IL, Ord VA. Orientation of tendons in the magnetic field and its effect on T2 relaxation times. Radiology 1985;155:433–5. https://doi.org/10.1148/radiology.155.2.3983395.
[62] Erickson SJ, Prost RW, Timins ME. The "magic angle" effect: background physics and clinical relevance. Radiology 1993;188:23–5. https://doi.org/10.1148/radiology.188.1.7685531.
[63] Du J, Pak BC, Znamirowski R, Statum S, Takahashi A, Chung CB, et al. Magic angle effect in magnetic resonance imaging of the Achilles tendon and enthesis. Magn Reson Imaging 2009;27:557–64. https://doi.org/10.1016/j.mri.2008.09.003.
[64] Lange T, Knowles BR, Herbst M, Izadpanah K, Zaitsev M. Comparative T2 and T1ρ mapping of patellofemoral cartilage under in situ mechanical loading with prospective motion correction. J Magn Reson Imaging 2017;46:452–60. https://doi.org/10.1002/jmri.25574.
[65] Wheaton AJ, Casey FL, Gougoutas AJ, Dodge GR, Borthakur A, Lonner JH, et al. Correlation of T1ρ with fixed charge density in cartilage. J Magn Reson Imaging 2004;20:519–25. https://doi.org/10.1002/jmri.20148.
[66] Nishioka H, Hirose J, Nakamura E, Oniki Y, Takada K, Yamashita Y, et al. T 1ρ and T 2 mapping reveal the in vivo extracellular matrix of articular cartilage. J Magn Reson Imaging 2012;35:147–55. https://doi.org/10.1002/jmri.22811.
[67] Jobke B, Bolbos R, Saadat E, Cheng J, Li X, Majumdar S. Mechanism of disease in early osteoarthritis: application of modern MR imaging techniques - a technical report. Magn Reson Imaging 2013;31:156–61. https://doi.org/10.1016/j.mri.2012.07.005.
[68] Van Tiel J, Kotek G, Reijman M, Bos PK, Bron EE, Klein S, et al. Is T1rho mapping an alternative to delayed gadolinium-enhanced MR imaging of cartilage in the assessment of sulphated glycosaminoglycan content in. Radiology 2016;279:523–31.
[69] Li X, Han ET, Ma CB, Link TM, Newitt DC, Majumdar S. In vivo 3T spiral imaging based multi-slice T1ρ mapping of knee cartilage in osteoarthritis. Magn Reson Med 2005;54:929–36. https://doi.org/10.1002/mrm.20609.
[70] Rauscher I, Stahl R, Cheng J, Li X, Huber MB, Luke A, et al. Meniscal measurements of T1 p and T2 at MR imaging in healthy subjects and patients with osteoarthritis. Radiology 2008;249:591–600. https://doi.org/10.1148/radiol.2492071870.
[71] Jerban S, Szeverenyi N, Ma Y, Guo T, Namiranian B, To S, et al. Ultrashort echo time MRI (UTE-MRI) quantifications of cortical bone varied significantly at body temperature compared with room temperature. Investig Magn Reson Imag 2019;23:202. https://doi.org/10.13104/imri.2019.23.3.000.
[72] Szomolanyi P, Rohrich S, Frollo I, Juras V, Schreiner M, Heule R, et al. Evaluation of compression properties of human knee cartilage-In-vivo study at 7T MRI. 2017 11th. Int Conf Meas Meas 2017:185–8. https://doi.org/10.23919/MEASUREMENT.2017.7983567. 2017 - Proc.
[73] Byra M, Wu M, Zhang X, Jang H, Ma Y-JJ, Chang EY, et al. Knee menisci segmentation and relaxometry of 3D ultrashort echo time cones MR imaging using attention U-net with transfer learning. Magn Reson Med 2020;83:1109–22. https://doi.org/10.1002/mrm.27969.